Dynamic Stress and Strain Analysis for 8x4 Truck Frame

Nagwa Ahmed Abdel-Halim

Dynamic Stress and Strain Analysis for 8x4 Truck Frame

Nagwa Ahmed Abdel-halim[1,a]

1 – Automotive Engineering Department, Faculty of Engineering, Mataria, Helwan University, Cairo, Egypt

a – Nagwaibrahim2006@yahoo.co.uk

DOI **10.13140/RG.2.1.3829.3363**

Keywords: 8x4 trucks, king pin inclination, camber, caster, toe-in, truck dynamics, dynamic chassis stress and strain, finite element models and analysis.

ABSTRACT. The truck chassis is subjected to lower stresses in rest than it is in movement where the stresses and strains are considerably increased. The current work contains the load cases and boundary conditions for stresses and strains analysis of chassis using finite element analysis. King pin inclination, camber, caster, and toe-in angles of a truck's wheels affect its chassis' longitudinal and transverse stresses and strains. This work concentrates on studying the chassis' stresses and strains when the truck is in longitudinal acceleration motion on asphalted straight road and has adjustable wheel angels for the steerable axles' wheels.

1. Introduction. Today wheel alignment is more sophisticated as there are several angles. Therefore, it is important to study the effect of wheel alignment as a factor on the truck chassis stresses and strains. Wheel alignment is often the cause of or at least a contributing factor in changes in the vehicle wheel forces, which is reflected on the values of chassis stresses and strains.

The stress analysis of chassis has been studied using finite element analysis over ANSYS in static and dynamic cases. Shell elements for the longitudinal and cross members, spring elements for suspension, and wheel stiffness have been used. In addition, impact loads have been measured experimentally. The road shocks and the vehicle moving situation have been studied with the adjacent corner of the frame. In addition, the determination of the natural frequencies of the chassis structure has been carried out by using Algor FEMPRO [1-4].

The previous studies investigated many kinds of classical and simple boundary conditions without considering wheel alignment as a factor of the chassis forces [1]. With the present approach, the study of the effect of the steerable wheels' adjustable angles was covered using finite element approach with MATLAB package, which is more efficient and simple. Also, general boundary conditions for the road in addition to most real conditions have been considered in this comprehensive model for the investigation of chassis stresses and strains.

2. Basic Concepts

A Mitsubishi FUSO truck, model S52JS4RFAB has been studied in static case after calculated its wheels reaction forces. The truck chassis finite element models were checked in static case for stiffness, deflection, shear and bending stresses, and strain by using MALAB software [5, 6].

In dynamic case, the truck chassis forces are varied under the variation in operation condition. In this study, the structural, construction, and material of the truck tires, and the side air resistance are neglected. Also, the study has been considered the truck's movement is a free rolling case and it moves on straight, hard, and dry road. This study is included the tire alignment as an effected parameter on the frame force.

2.1 Influence of Wheel Angles on the Location of Axle Loads [7-9]

The adjusting of the steered wheels' angles is very important to keep the conditions for optimum steer of a vehicle. In addition, it makes the vehicle follows a path which is part of the circumference of its turning circle, which will have a center point somewhere along a line extending the axis of the fixed axle. It keeps the steered wheels at 90 degrees to a line drawn from the circle center through the center of the wheel as represents in Fig. 1 (a), (b).

To show the tire forces in three axes; longitudinal force F_x (x-axis), vertical load F_y (y-axis), and lateral force F_z (z-axis), which can be acting on the center of tire contact a zoomed in picture of a one tire, is shown in Fig. 2.

For static case, the positive kingpin inclination results a moment ($M_{yk}=F_y w_w/2$) around the wheel axis when the vertical wheel load (F_y) is shifted to the wheel axis and resolved into two components $F_y sin\beta$ (perpendicular on the king pin) and $F_y cos\beta$ (parallel to the king pin) as shown in Fig. 3.

A lateral force (F_z) will be created due to the vehicle wheel cambered at its top towards the outside by angle (Φ). The reaction force ($F_{z,c}$) of the lateral force (F_z) will be appeared at the wheel axis. The reaction force ($F_{z,c}$) will be resolved into two components $F_{z,c}\ cos\beta$ (perpendicular on the king pin) and $F_{z,c}\ sin\beta$ (parallel to the king pin) as shown in Fig. 4.

The toe-in angle (α) is that results from change the distance between the vehicle center plane in the longitudinal direction and the line intersecting the center plane of one wheel with the road plane and this angle (α) corresponds to the tire slip angle. Fig. 5, 6 represent the plane view of the tire toe-in angle with the kingpin inclination and the tire toe-in, tire camber with the kingpin inclination. Equations 1, 2 describe the forces, which are shown at the center of wheel in Fig. 6.

Fig. 7 details the positive caster angle (τ). It is the angle between the steering axis (EG) projected onto a xy-plane and a vertical drawn through the wheel center. Also, it clears that the kinematic caster trail ($r_{t,k}$), the lateral force trail ($r_{t,T}$), dynamic radius (r_{dyn}), the force F_{yz}, and its components F_{yzvk}, F_{yzhk} which are in equations (3-5).

Fig. 8 shows the plane view of Fig 7. This figure shows how the center of the lateral forces (F_{zwA}) moves back by the value of the kinematic caster trail ($r_{t,\tau}$). While the longitudinal forces (F_{xwA}) moves outside by the camber offset (r_t). Equations 6, 7 contain the values of the above forces.

$$Fcsc = Fz\ ccos\beta - Fy\ sin\beta \quad (1)$$

$$Fccs = Fy\ cos\beta + Fz\ csin\beta \quad (2)$$

$$Fyz = Fccs \quad (3)$$

$$Fyzvk = Fccs\ sin\tau \quad (4)$$

$$Fyzpk = Fccs\ cos\tau \quad (5)$$

$$FzwA = Fcsc \quad (6)$$

$$FxwA = Fyzvk \quad (7)$$

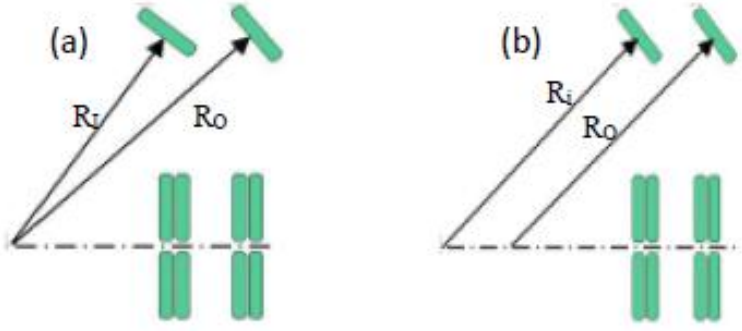

Fig.1. Steering geometry (a) with positive, (b) with zero tire rod angle

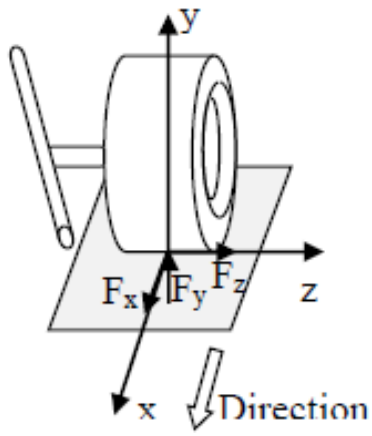

Fig. 2. The tire forces in three axes

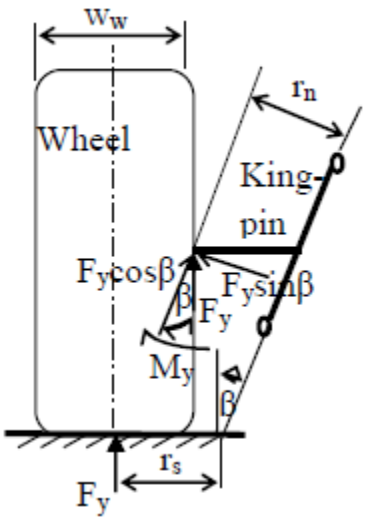

Fig. 3. Side view of the kingpin inclination

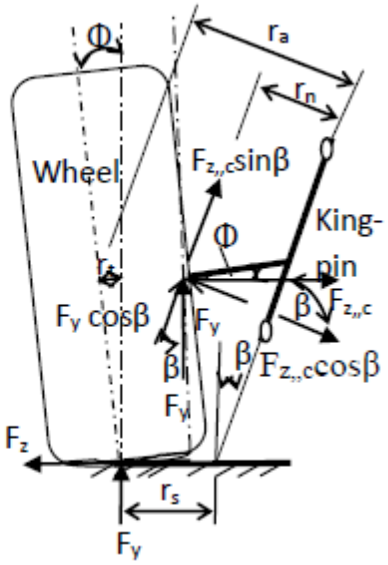

Fig. 4. Side view of camber with kingpin inclination

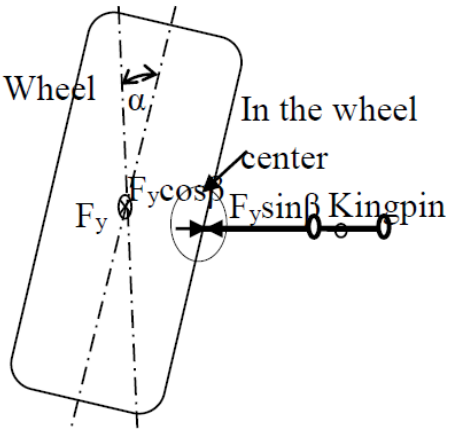

Fig. 5. Plan view of tire toe-in with kingpin inclination

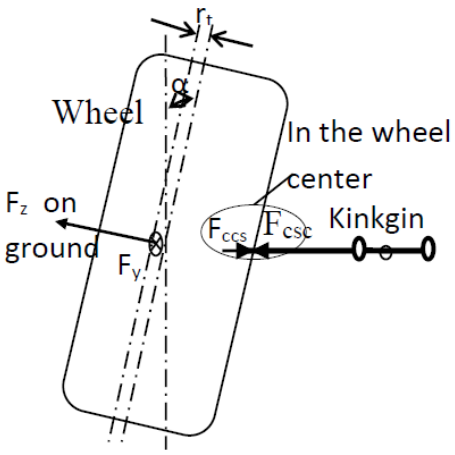

Fig. 6. Plan view of tire camber with toe-in and kingpin inclination

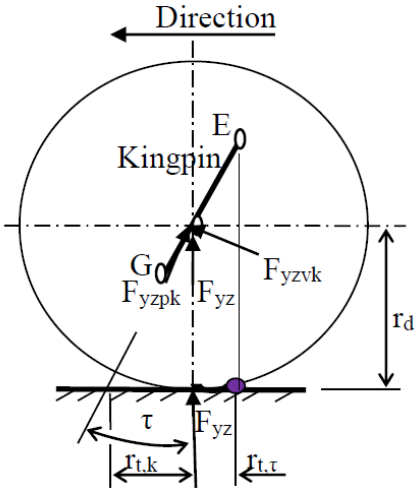

Fig. 7. Side view of the tire with positive caster angle

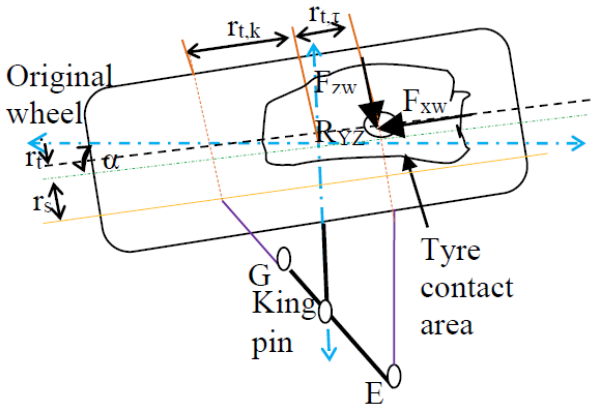

Fig. 8. Plan view of tire with all tire angles

2.2 Truck Chassis Dynamic Model [5, 10-13].

The truck used for the study is accelerating on the level ground by acceleration (a). The forces of inertia F_{in}, air resistance F_{air}, and rolling resistance F_r of the progressively moving masses directed oppositely to the acceleration. The truck chassis dimensions and forces in dynamic case are viewed in Fig. 9. The longitudinal forces at the wheels contact point with the ground *A*, *B*, *C*, *D* can be

computed by sequence of steps. Firstly, the equation of motion along the longitudinal axis of the truck according the force balance method is expressed by equation 8 whereas the front axles' tractive effort is zero because the truck is a rear wheel drive. The tractive effort for the rear axles is calculated as the equations group 9 and the dynamic wheel radius can be determined from equation 10. Secondly, the summation of air, rolling, coefficient of rolling resistance, and inertia resistance forces for the truck components mention in equations (11-14). Thirdly, the distribution of both the inertia and air resistance forces on the contact points of the truck's wheels with the ground can be made by; a) Calculate the percentage of a vertical load of a truck wheel related to the summation the vertical loads of all wheels (equation 15). b) Multiply the percentage of the wheel load and the summation for both the inertia and air resistance forces (group of equations 16). C) Sum the resistance forces at the wheel contact point (group of equations 17).

$$md^2x/dt^2 = aW/g = F_{TC} + F_{TD} - \Sigma R_r - \Sigma R_{air}$$

$$F_{TC} + F_{TD} \geq \Sigma(R_{in} + R_r + R_{air}) \quad (8)$$

$$F_{TC} = M_{emax}\, i_{gn} i_{f1} \eta_t / n_{w1} r_d,\ F_{TD} = F_{TC} i_{f2} \quad (9)$$

$$r_d = 0.5D_r + B_t(1-\lambda_t) \quad (10)$$

$$\Sigma R_{air} = KaB_aHaV^2 \quad (11)$$

$$\Sigma R_r = f\,(R_{YZA} + R_{YZB} + R_{YZC} + R_{YZD}) \quad (12)$$

$$f = f_0\,(1 + V^2_{max}/1500)\ (V \text{ by m/s}) \quad (13)$$

$$\Sigma R_{in} = a/g(\Sigma w) = (\Sigma w) =$$

$$F_{in1}+F_{in2}+F_{incc1}+F_{in3}+F_{incc2}+F_{in4}+F_{in5}+F_{in6}+F_{incc3}+F_{in7}+F_{inc4}+F_{in8} \quad (14)$$

$$\%\, R_{YZA} = R_{YZA} / \Sigma\,(R_{YZA} + R_{YZB} + R_{YZC} + R_{YZD}) \quad (15)$$

$$(R_{inA}+R_{airA}) = \Sigma(R_{in} + R_{air}) \cdot \%\, R_{YZA},$$

$$(R_{inB}+R_{airB}) = \Sigma(R_{in} + R_{air}) \cdot R_{YZB},$$

$$(R_{inC}+R_{airC}) = \Sigma(R_{in} + R_{air}) \cdot \%\, R_{YZC},$$

$$(R_{inD}+R_{airD}) = \Sigma(R_{in} + R_{air}) \cdot \%\, R_{YZD} \quad (16)$$

$$F_A = fR_A + R_{inA} + R_{airA},\ F_B = fR_B + R_{inB} + R_{airB},\ F_C = fR_C + R_{inC} + R_{airC},\ F_D = fR_D + R_{inD} + R_{airD} \quad (17)$$

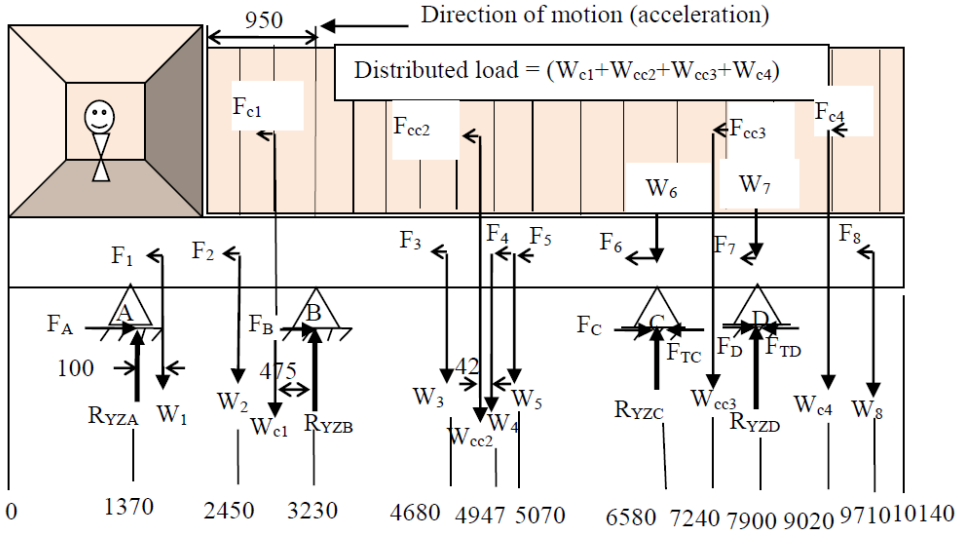

(a)

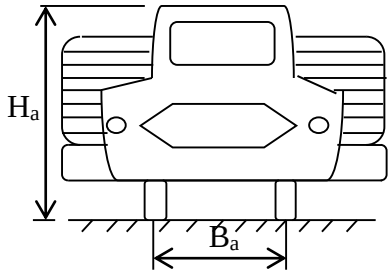

(b)

Fig. 9. (a) The truck chassis dimensions and forces in dynamic case, (b) head area of the truck

2.3 Influence of Wheel Angles on the Value of Axle Loads [7, 8].

The truck chassis was modeled to study the effect of the wheel angles on the value of vertical reaction, longitudinal, and transverse (lateral) forces. From that point of view the vertical forces at the wheels contact points will be changed for the two front steered axles but didn't change for the two rear drive axles to be become as in equations (18-21). From that and the above paragraph the longitudinal forces at points *A, B, C, D* will be as illustrated in equations (22-25). The average lateral force results from the wheel camber on the dry road F_z is represented in equation 26. Therefore, the lateral force at points *A, B, C, D* are illustrated through equations (27-30).

$$R_{YZA} = R_A cos\beta + F_{z,,c} sin\beta \quad (18)$$

$$R_{YZB} = R_B cos\beta + F_{z,,c} sin\beta \quad (19)$$

$$R_{YZC} = R_C \quad (20)$$

$$R_{YZD} = R_D \quad (21)$$

$$F_A = F_{xwA} = f\, R_{YZA} + cos\beta\, (R_{inA} + R_{airA}) \quad (22)$$

$$F_B = F_{xwB} = f\, R_{YZB} + cos\beta\, (R_{inB} + R_{airB}) \quad (23)$$

$$F_C = F_{xwC} = f\, R_{YZC} + (R_{inC} + R_{airC}) \quad (24)$$

$$F_D = F_{xwD} = f\, R_{YZD} + (R_{inD} + R_{airD}) \quad (25)$$

$$F_z = F_{z.c} = F_{zw} = F_y \sin \Phi \quad (26)$$

$$F_{zwA} = R_{yzA} \sin \Phi = R_A (cos\beta + sin\beta) \sin \Phi \quad (27)$$

$$F_{zwB} = R_{yzB} \sin \Phi = R_B (cos\beta + sin\beta) \sin \Phi \quad (28)$$

$$F_{zwC} = R_C f_t \quad (29)$$

$$F_{zwD} = R_D f_t \quad (30)$$

3. The Finite Element Model of the Truck Chassis [6, 14-15].

In this study the FEA has been used to analysis the truck chassis beams strength in dynamic case. The same procedure in reference [6] could be repeated. However the truck chassis's beam model forces and supports reactions could be located at the same places but in three dimension axes. And also, the number of elements is five hundred; each element has nearly twenty mm (20.28 mm) length with two nodes at its edges.

3.1 Global Stiffness Matrix (K_{NgNg}) and The Deflection Vector (δ_{NgNg}).

The shape of the element stiffness matrix in three dimensions is completely different rather than in one dimension. Each node in this case study has five degrees of freedom namely longitudinal (u), vertical (y), lateral (l) displacements respectively and xy-plane cross-section (slope) rotation (Θ_z), xz-plane cross-section (slope) rotation (Θ_y) respectively. The linear system for Euler-Bernoulli beam has been described in equation 31, 32 for one element (L) as a complete element stiffness matrix (Kij), nodal variables (displacements and rotations) vector (δe), and nodal force vector (Fe). Matrix 32 is the element equilibrium equations for a two-plane bending element with axial stiffness in matrix form. The axial [K_{axial}], bending $[K_{bending}]_{xy}$, and bending $[K_{bending}]_{xz}$ stiffness matrices are detailed in appendix 1. The calculation steps of the assembled stiffness matrix (K_{NgNg}), and the assembled deflection vector ($\boldsymbol{\delta}_{NgNg}$) is nearly as reference [6] with difference in the size of the global stiffness matrix.

$$[K_{ij}] \cdot [\delta e] = [F_e] \tag{31}$$

$$\begin{bmatrix} [K_{axial}] & [0] & [0] \\ [0] & [K_{bending}]_{xy} & [0] \\ [0] & [0] & [K_{bending}]_{xz} \end{bmatrix} \begin{bmatrix} u_1 \\ u_2 \\ v_1 \\ \theta z_1 \\ v_2 \\ \theta z_2 \\ l_1 \\ \theta y_1 \\ l_2 \\ \theta y_2 \end{bmatrix} = \begin{bmatrix} fx_1 \\ fx_2 \\ fy_1 \\ Mz_1 \\ fy_2 \\ Mz_2 \\ fz_1 \\ My_1 \\ fz_2 \\ My_2 \end{bmatrix} \tag{32}$$

3.2 Stresses and Strains for the Truck Chassis in Three Axes.

In this article, Galerkin's method is used in stress analysis of the truck chassis in three dimensions. The truck chassis elements have been loaded tensional-compression in the x direction. From elementary strength of materials theory, the $\mathcal{E}_x$ represents the strain resulting from applied load while the induced strain components are given by $\mathcal{E}_y = \mathcal{E}_z = - \nu \mathcal{E}_x$. Equations 33, 34 resulted from strength of materials' laws for tension load and the substitution in the general stress-strain relations. This study has been assumed two planes of stress, that xy and xz planes. When xy is the plane stress, $\sigma_b(xy)$, $\mathcal{E}_y$, and τ_{xy} can be calculated from equations (35-38). Again, by assuming that the xz plane is the plane stress, $\sigma_b(xz)$, $\mathcal{E}_z$, and τ_{xz} can be calculated from equations (39-42).

$$\sigma_{t,c} = F(x)/A \tag{33}$$

$$\mathcal{E}_x = \sigma_{t,c} / E \tag{34}$$

$$\sigma_b(xy) = M(xy)*D/2I_z \tag{35}$$

$$\mathcal{E}_y = ((1+\nu)(1-2\nu)\sigma_b(xy) - \nu\sigma_{t,c}) / E(1-\nu) \tag{36}$$

$$\tau_{xy} = (F(y)BD^2) / (8I_z b) \tag{37}$$

$$\gamma_{xy} = \tau_{xy}/(E/(2(1+\nu)) = \tau_{xy}/G \tag{38}$$

$$\sigma_b(xz) = 6M(xz)/(D(B^2+(b/B)-1)-2b((b/B)-1)) \tag{39}$$

$$\mathcal{E}_Z = ((1-2\nu)/E(1-\nu))((1+\nu)\sigma_b(xz) - (\nu/(1-\nu)((1+\nu)\sigma_b(xy) + \sigma_{t,c}) \tag{40}$$

$$\tau_{xz} = (F_Z B^2 D) / (16 I_Y b) \tag{41}$$

$$\gamma_{xz} = \tau_{xz} / G \tag{42}$$

4. Results and Discussions of Truck Chassis's stresses and strains.

The vertical loads (w_1…….etc) and reaction forces on the wheels (R_A…….) for one side of the chassis in static case have been written in Table 1. The wheel angles for the two front truck axles' wheels have been taken equally while the two rear axles' wheels haven't adjustable angles. The values of the front wheels angles summarized in Appendix 2 Table 2. Appendix 2 also contains Tables 3, Table 4. Table 3 includes the variables' values for the variables of paragraph (2.2). Table 4 has the longitudinal and lateral forces' names and their values on one side of the truck chassis. All the Table in Appendix 2 has been used in drawing the stresses and strains graphs. Fig. 10, 11 represent the tension-compression stress and strain respectively. Fig. 12, 13 shows the vertical bending stress and strain respectively. Fig. 14, 15 have the vertical shear stress and strain respectively. The drawing in Fig. 16, 17 have the lateral bending stress and strain respectively. The lateral shear stress and strain have been represented through Fig. 18, 19 respectively. Each couple of the above figures has the same trend but with difference in their values. As example the maximum value of the lateral shear stress is about 36 N/mm^2 while the maximum of the lateral shear strain is about $44\text{x}10^{-5}$ and so on for the others couples.

Summary. The noticed from this study is the wheel angles generate lateral force. Although the generated lateral force causes lateral stress on the frame chassis, it will help for smooth turning of the truck. Also, the noticed from the graphs 16, 17 that they have completely different trend in the shapes oppositely the others stresses and strains coupled graphs.

In this search, the description of the truck's accelerating motion on flat, asphalted, and smooth road generate valuable longitudinal stress whenever the maximum value its maximum value is 24 N/mm^2.

This article considered a compromise of using the Finite Element Techniques (FET), MATLAB package; studying the effect of the steerable wheels' angles on truck frame's forces values and direction, analyze the forces, which result from the truck dynamic motion.

Finally, the article includes many drawings for the stresses and strains in *x*-axis, *xy* plane stress and *xz* plane stress.

Nomenclature

F_x – Wheel longitudinal force
F_y – Wheel vertical load or R_A or R_B or R_C or R_D
F_z – Lateral force due to wheel cambered
$F_{z,c}$ – Reaction force of the lateral force
$F_{z,t}$ – Summation of the lateral forces
$F_{x,t}$ – Summation of the longitudinal forces
F_{TC} – Tractive effort of one wheel of the first rear axle
F_{TD} – Tractive effort of one wheel of the second rear axle
R_A, R_B, R_C, R_D – Vertical truck wheels reaction forces before adding the effect of wheel angles
R_{YZA}, R_{YZB}, R_{YZC}, R_{YZD} – Vertical truck wheels reaction forces after adding the effect of wheel angles
R_{air} – Air resistance
R_{in} – Inertia resistance
d^2x/dt^2 or (a= 5.5 m/s^2) – Linear acceleration of the truck
g – Acceleration due to gravity
μ – Constant ((a/g) =0.56)
M_{emax} – Engine maximum torque (1770 N m at 1100 rpm)
i_{gn} – The gearbox reduction ratio
i_{f1} – The first differential reduction ratio (2.15)
i_{f2} – The second differential reduction ratio (2.15)
η_t – The drive line efficiency (0.9)
n_{w1} – Number of wheels on the first rear axle (4)
r_s – Wheel static radius
$\%\ R_{YZA}$ – Percentage vertical reaction force at point A
R_{inA}, R_{airA} – Inertia and air resistances at point A
R_r – Rolling resistance
F_{in1} ……..F_{in8} – Inertia forces for the truck components
w_w – Tire width
r_n – Distance between the steering axis to the vertical wheel load at the wheel center
r_s – Kingpin offset
β – Kingpin inclination angle
Φ – Wheel camber angle
r_a – Longitudinal force lever depends on the kingpin offset
r_t – Camber offset
α – Toe-in angle
τ – Caster angle
$r_{t,k}$ – Caster trail
$r_{t,T}$ – Lateral force trail
r_{dyn} – Dynamic radius
m – Truck mass (kg)
$M(xy)$ – Moment in xy plane
$M(xz)$ – Moment in xz plane
$\sigma_b(xy)$ – Bending moment in xy plane
ε_y – Strain in xy plane

r_d – Wheel dynamic radius
D_r – Diameter of wheel rim, m
B_t – Height of tire profile in a free state, m
λ_t – Radial deformation coefficient of the tire
K_a – Air resistance coefficient N.S^2/m^4
B_a – Track in m
H_a – Maximum height of the automobile in m
V – Maximum truck speed (80 km/hr)
f_0 – Longitudinal rolling resistance coefficient at a low speed (0.018)
f – Longitudinal rolling resistance coefficient at a maximum speed
f_t – Transverse rolling resistance coefficient at a maximum speed ≈ f
γ – Poisson's ratio

τ_{xy} – Shearing stress is acting in the direction of the x axis on a surface perpendicular to the y axis (N/mm^2)
γ_{xy} – Shear strain is in xy plane (N/mm^2)
$\sigma_b(xz)$ – Bending moment in xz plane (N/mm^2)
ε_Z – Strain in xz plane
τ_{xz} – Shearing stress in xz plane (N/mm^2)
γ_{xz} – Shear strain is in xz plane (N/mm^2)
G – Shear modulus
L – Finite element length (mm)
$\sigma_{t,c}$ – Tension-compression stress
A – Chassis cross section area (mm^2)
E – Modulus of elasticity N/mm^2
I_z – Modulus of section related to z axis
I_y – Modulus of section related to y axis
D – Cross section height (mm)
B – Cross section web (mm)
b – Cross section thickness (mm)

Appendix 1

The axial [K_{axial}], bending $[K_{bending}]_{xy}$, and bending $[K_{bending}]_{xz}$ stiffness matrices are:

$$[K_{axial}] = (AE/L)\begin{bmatrix} 1 & -1 \\ -1 & 1 \end{bmatrix}$$

$$[K_{bending}]_{xy} = (EI_z/L^3)\begin{bmatrix} 12 & 6L & -12 & 6L \\ 6L & 4L^2 & -6L & 2L^2 \\ -12 & -6L & 12 & -6L \\ 6L & 2L^2 & -6L & 4L^2 \end{bmatrix}$$

$$[K_{bending}]_{xz} = (EI_y/L^3)\begin{bmatrix} 12 & -6L & -12 & -6L \\ -6L & 4L^2 & 6L & 2L^2 \\ -12 & 6L & 12 & 6L \\ -6L & 2L^2 & 6L & 4L^2 \end{bmatrix}$$

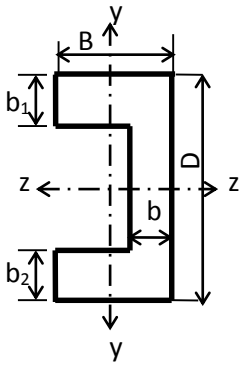

Fig. (A-1). Channel Cross Section Area ($b=b_1=b_2$)

Appendix 2

Chassis components Loads, reactions, and resistances forces in static and dynamic cases for one side of the truck chassis:

Table 1. One Side Vertical Loads of Chassis's Truck and wheels Angles

Without Wheel Angles	***Without Wheel Angles***
Loads Name Values (N)	***Loads Name Values (N)***
w_1 39208.3	w_8 245.5
w_2 2526.1	$R_A = F_y$ at wheel (A) 35177
w_{c1} 6453.8	$R_B = F_y$ at wheel (B) 27599
w_3 981	$R_C = F_y$ at wheel (C) 7777
w_{cc2} 22758	$R_D = F_y$ at wheel (D) 29661
w_4 1471.5	***With Wheel Angles***
w_5 1895.5	***Loads Name Values (N)***
w_6 245.5	R_{yzA} 34840.3
w_{cc3} 8967.3	R_{yzB} 27323
w_7 245.5	$R_{yzc} = R_C$
w_{c4} 15217.3	$R_{yzD} = R_D$

Table 2. Wheel Angles Symbols and Values

β	9 º	Φ	1 º	α	0.1 º	τ	1 º

Table 3. Values for the Variables of Paragraph (2.2)

Sy.	Value	Sy.	Value	Sy.	Value	Name	Value
λ_t	0.2	B_t	0.236 m	Ka	0.7Ns^2/m^4	$R_{inC}+R_{air\ C}$	4539 N
f_0	0.018	r_d	0.47 m	ΣR_{in}	56121 N	$R_{inD}+R_{air\ D}$	17341 N
f	0.024	H_a	3.24 m	ΣR_{yz}	99601 N	Without angles	
$\%R_{yzA}$	35	B_a	1.85 m	ΣR_{air}	2072 N	F_A	21212 N
$\%R_{yzB}$	27.4	r_s	0.522 m	$\Sigma(R_{in}+R_{air})$	58193 N	F_B	16607 N
$\%R_{yzC}$	7.8	D_r	0.572 m	$R_{inA}+R_{air\ A}$	20367 N	F_C	4725.6 N
$\%R_{yzD}$	29.8	D_r	0.572 m	$R_{inB}+R_{air\ B}$	15945 N	F_D	18053 N

Values for the Variables of stresses and Strains Equations							
γ	0.3	B	90 mm	A	3262 mm^2	I_z	40.69*10^6 mm^4
D	300 mm	b	7 mm	E	2.1*10^5 N/mm^2	I_Y	45.97*10^5 mm^4

Table 4. Longitudinal and Lateral Forces on One Side of Chassis's Truck

Longitudinal Force Value(N)	**Longitudinal Force Value(N)**
$F_A = F_{xwA}$ 20953	$F_C = F_{xwC}$ 4726
$F1 = w_1\mu$ 21957	F_{TC} 26236
$F2 = w_2\mu$ 1415	$F_6 = w_6\mu$ 137
$F_{c1} = w_{c1}\mu$ 3614	$F_{cc3} = w_{cc3}\mu$ 5022
$F_B = F_{xwB}$ 16404	$F_D = F_{xwD}$ 18053
$F_3 = w_3\mu$ 549	F_{TD} 56407
$F_{cc2} = w_{cc2}\mu$ 12744	$F_7 = w_7\mu$ 137
$F_4 = w_4\mu$ 824	$F_{c4} = w_{c4}\mu$ 8522
$F_5 = w_5\mu$ 1061	$F_8 = w_8\mu$ 137
Lateral Force Value(N)	**Lateral Force Value(N)**
F_{zwA} 610	F_{zwC} 187
F_{zwB} 478	F_{zwD} 712

Appendix 3

The longitudinal, vertical, lateral stresses and strains.

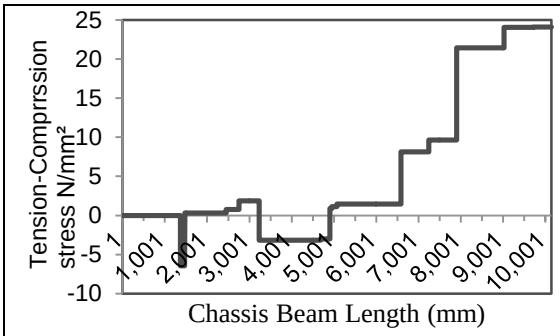

Fig. 10. Tension-Compression Stress versus Chassis Beam Length

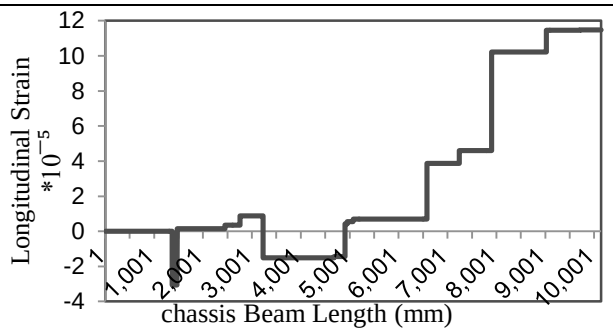

Fig. 11 Longitudinal Strain versus Chassis Beam Length

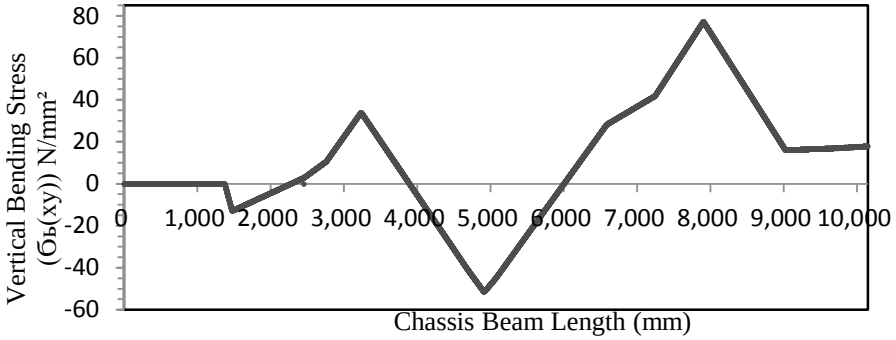

Fig. 12. Vertical Bending Stress versus Chassis Beam Length

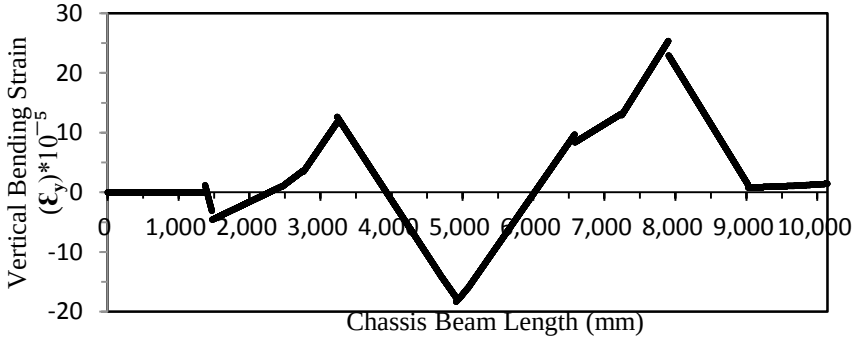

Fig. 13. Vertical Strain versus Chassis Beam Length

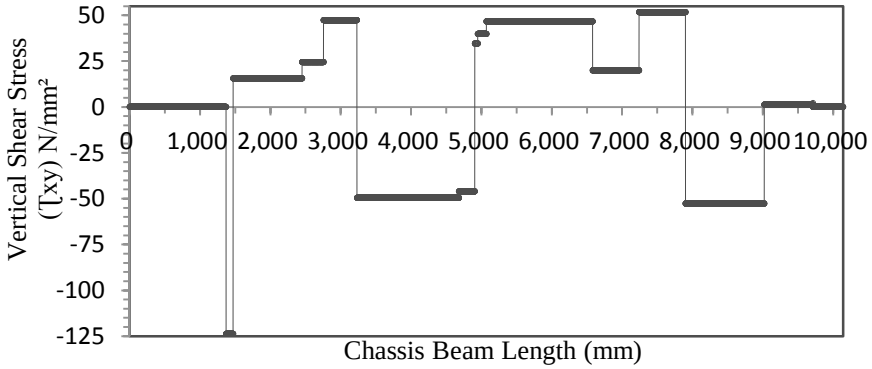

Fig. 14. Vertical Shear Stress versus Chassis Beam Length

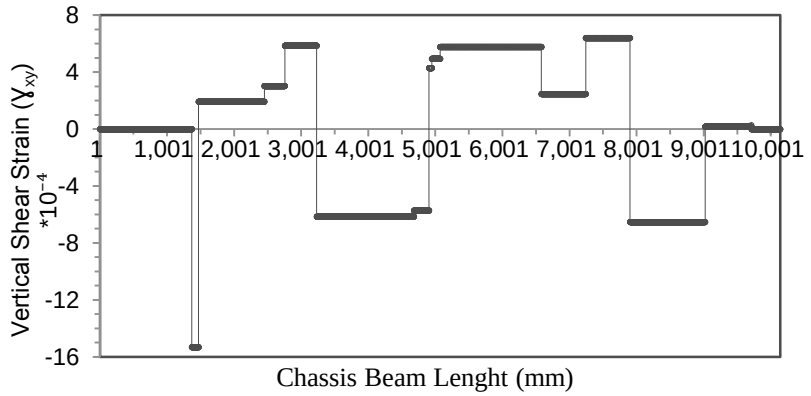

Fig. 15. Vertical Shear Strain versus Chassis Beam Length

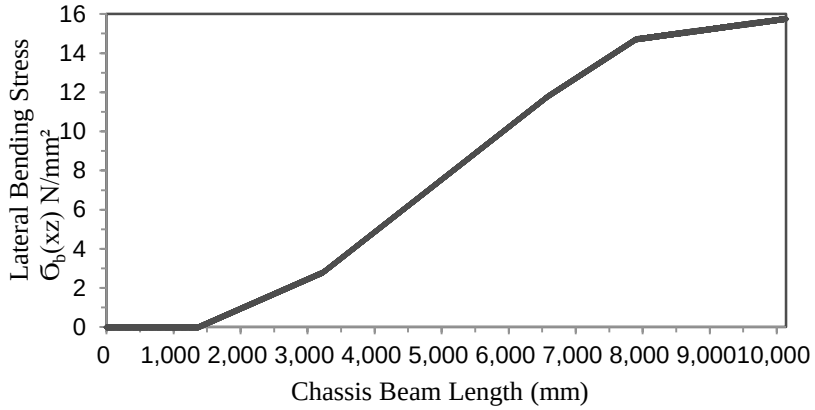

Fig. 16. Lateral Bending Stress versus Chassis Beam Length

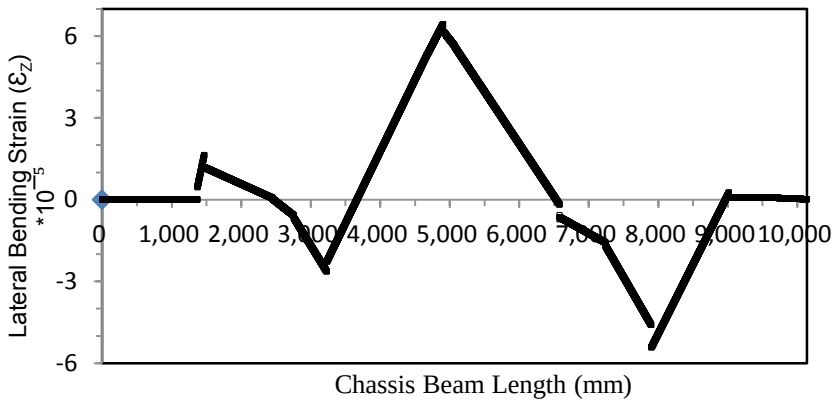

Fig. 17. Lateral Bending Strain versus Chassis Beam Length

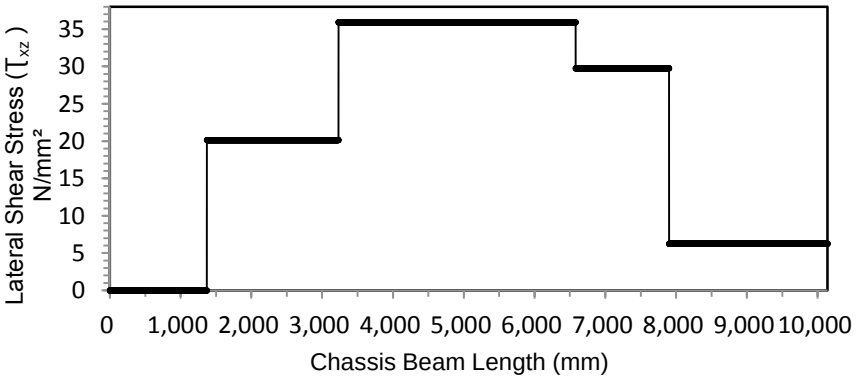

Fig. 18. Lateral Shear Stress versus Chassis Beam Length

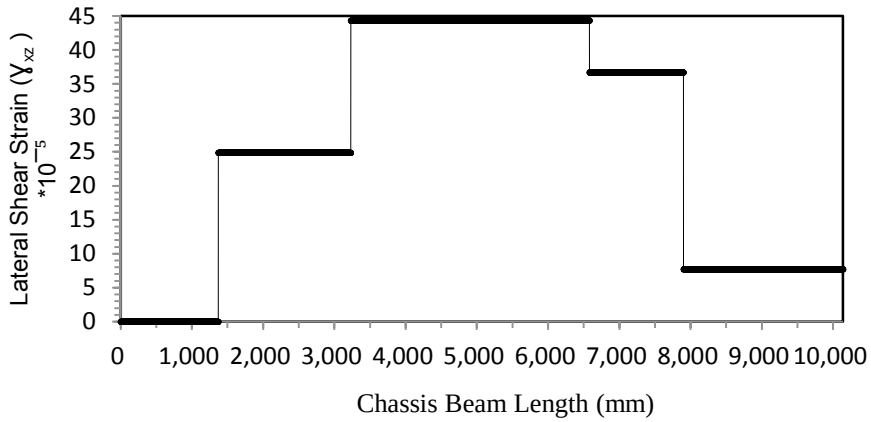

Fig. 19. Lateral Shear Strain versus Chassis Beam Length

References

[1] Teo Han Fui, Roslan Abd. Rahman (2007) 'Statics and Dynamics Structural Analysis of A 4.5 Ton Truck Chassis', Jurnal Mekanikal, No. 24, PP. 56-67.

[2] Ashutosh Dubey and Vivek Dwivedi (2003) 'Vehicle Chassis Analysis: Load Cases & Boundary Conditions for Stress Analysis'.

[3] Dheeraj S.and Sabarish R. (2014) 'Analysis of Truck Chassis Frame Using FEM', Middle-East Journal of Scientific Research 20(5), ISSN 1990-9233, PP. 656-661.

[4] Sani M. S. M., Arbain M. T. and et al (2009) 'Stress Analysis and Modal Transient Response of Car Chassis', International Conference on Advance Mechanical Engineering (ICAME09), 22-25 June 2009. Shah Alam, Selangor.

[5] Abdel-halim Nagwa A. (2015) 'Reflection of Truck Loads Distribution Methods on the Truck Wheels Reaction Forces', American Journal of Engineering, Technology and Society, Issue 4, Vol. 2, Pages 67-76.

[6] Abdel-halim Nagwa A., Abdel-hafiz Mohamed M. M. (2015) 'Stress and Strain Analysis for a Ladder Truck Chassis', American Journal of Engineering, Technology and Society, Issue 6, Vol. 2, Pages 131-139.

[7] Dana Spicer, (2007) 'Steer Axles Application Guidelines", AXAG0400, PP. 1-46.

[8] Prof. Dipl.-Ing. Jornsen Reimpell and Dipl.-Ing. Helmut Stoll (1996) 'The Automotive Chassis: Engineering Principles, Types of drive and suspension, Tyres and wheels, Axle kinematics, steering, Springing, Chassis and vehicle overall', English edition, Arnold London.

[9] van Berkum A. (2006) Chassis and suspension design FSRTE02, Unpublished Master's Thesis, Technische Universiteit Eindhoven, Department of Mechanical Engineering, Section Dynamics and Control Technology.

[10] Artamonov M. D., Ilarionov V. A., and Morin M. M. (1976) 'Motor Vehicles: Fundamentals and Design', Mir bublishers Moscow.

[11] Wong J. Y.(1978) 'Theory of Ground Vehicles', A Wiley New York.

[12] Mehdi Mahmoodi-k, Iraj Davoodabadi, and et al (2014) 'Stress and Dynamic Analysis of Optimized Trailer Chassis', Technical Gazette 21, 3, PP. 599-608.

[13] Mitsubishi Fuso Truck & Bus Corporation (2009) Heavy Duty Fuso FS52JS4RFAB, Part No. TSH58A www.fuso.com.au

[14] Hutton David V. (2004) 'Fundamentals of Finite Element Analysis', McGraw New York.

[15] Mahvi Malik Shahzad, ShaikhRizwan, Tarique khan (2015) 'Finite Element Static Structural Analysis of 4X2 Truck Chassis Frame', International Journal of Modern Trends in Engineering and Research, e-ISSN No.:2349-9745, Issue 7, Vol. 2, PP. 1909-19014. www.ijmter.com